1424 *Macromolecules* **2002,** *35,* 1424−1436

# Structure and Entropy of a Long Polymer Chain in the Presence of Nanoparticles

**Waldemar Nowicki**[†]

*Adam Mickiewicz University, Faculty of Chemistry, Grunwaldzka 6, 60-780 Poznań, Poland*

*Received January 11, 2001; Revised Manuscript Received August 24, 2001*

ABSTRACT: We describe a detailed study of the conformational properties of a very long polymer chain in the presence of small colloidal particles. The polymer chain is modeled by a random self-avoiding walk (SAW) on the cubic lattice. The properties of interest include the conformational entropy, segment distributions in the coil, and dimensions of the coiled chain attached to a particle. The conformational entropy of a coil perturbed by a nonadsorbing particle and by a particle attached to the chain end is calculated. The influence of the particle size on the minimum adsorption energy per surface unit of the particle, needed to outweigh the conformational entropy effect, is examined. The conformations of the free coil and the coil distorted by the irreversible adsorption of a particle are studied. On the basis of the results obtained, the possible structures of the particle-plus-polymer aggregates are discussed.

## 1. Introduction

The problem of adsorption of polymer chains on planar surfaces has been extensively studied and is well-understood.[1] The behavior of polymers on restricted dimensions and various geometries is less well-understood although it is important in practice.[2] The role of the surface curvature in polymer adsorption has been investigated in the context of adsorption on rough surfaces,[3−13] binding of surfactant micelles to macromolecules,[14,15] and interaction of polymers with colloidal particles.[16−27] The present work concerns the last case, that is, the polymer−particle interaction. In particular, it deals with the situation when the macromolecule size is significantly greater than that of particles. Various examples of such systems can be encountered in practice.[14,27−30]

The colloid−polymer interactions can modify the stability of colloidal suspensions. This phenomenon is of great practical importance in many biological, medical, environmental, and chemical industrial processes,[31−41] and therefore it attracts much scientific interest. There exists an extensive literature concerning the role of polymers in processes of stabilization and flocculation of suspensions. However, in the majority of cases, where the processes have been studied, the colloidal particles are large compared with the radii of gyration of polymers. The reverse case has received much less attention although the interactions between supersized polymers, and fine colloidal particles are important in water and wastewater purification[28,29] and paper manufacture.[30] These interactions are also important in biological systems.[14,27,42,43]

In systems containing supersized coils and fine colloidal particles, the adsorption process can produce multiplets, i.e., species built of a number of particles attached to a single polymer molecule.[14,17,44−48] The stability of such suspensions is determined by multiplet properties,[45−49] which depend—among other factors—on the particle-to-macromolecule number concentration ratio, the radius of the effective repulsion between particles, the initial conformation of the polymer, etc.[47−51] Although the chain conformation and the loss of its conformational entropy caused by the particle attachment are important factors determining the properties of multiplets, up to now attempts aiming a quantitative calculation of the conformational entropy of the polymer chain have been relatively few,[52] especially in the presence of colloidal particles.

Macromolecular coils in good solvents are very loose; the actual macromolecule occupies a few percent at most of the region of the coil.[53] In the case of poly(ethylene oxide) in water the volume of the chain itself represents <0.1% of the volume pervaded by the chain.[54] Therefore, very small objects like, for instance, micelles, colloidal particles of nanometer size, or protein globules, can easily enter the coil.[42] Nonetheless, the presence of such small impenetrable objects in the coil domain reduces the number of possible conformations of the polymer chain. The macromolecule adopts its conformation to the presence of the particle, which can lead to a disturbed distribution of segments in the coil and a decrease in the polymer entropy. In this study an approach is made to consider the effect of small colloidal particles on the structure of polymer coil and the coil conformational entropy, using a simple lattice model. Two cases are considered: the insertion of nonadsorbing particle into the coil domain and the irreversible attachment of one chain end to the particle. The results of the conformational entropy calculation are used to estimate the reversible adsorption energy per the surface unit of a particle needed to outweigh the loss of entropy caused by a restriction of the number of available configurations. Also, an attempt is made to predict the structure of particle-plus-polymer aggregates by means of the analysis of distributions of empty (i.e., not occupied by polymer segments) areas and adsorption sites for particles in the domain of the coil.

Since the conformational entropy of the coil perturbed by an object inserted into it is considered, let us first review briefly some approaches to the calculation of the conformational entropy of polymer chain.

The number of conformations of a SAW (self-avoiding walk) chain can be calculated using several techniques like the exact enumeration,[55] the renormalization group

---

[†] Tel 48-61-8291-457, fax 48-61-8658-008, e-mail gwnow@main.amu.edu.pl.

10.1021/ma010058d CCC: $22.00

(RG) theory,[56,57] and other approximate methods.[52,58] The RG theory provides a simple equation for the calculation of the number of conformations of the chain:[55,59]

$$\Omega_F = C_F N^{\gamma_F - 1} \mu_F{}^N \tag{1}$$

where $N$ is the number of segments. Symbols $C$ and $\gamma$ denote constants dependent on the lattice coordination number, and $\mu$ is the total effective coordination number of the lattice. For the cubic lattice we have $C_F = 1.17$,[60] $\gamma_F = {}^7/_6$, and $\mu_F = 4.6838$.[61] The subscript F refers to free polymer chains, whereas the subscript A, used below, is reserved for macromolecules adsorbed.

Equation 1 enables one to find the conformational entropy of a free polymer chain. Also, it allows the calculation of the entropy loss due to the attachment of one end of the chain to a wall.[62] Results of the numerical study presented in ref 62 have shown that the chain attachment only slightly affects the total effective coordination number, and it can be assumed that $\mu_A = \mu_F$, as was deduced theoretically by Whittington.[63] Also, the difference between $\gamma_F$ and $\gamma_A$ values is found to depend on the lattice dimensionality only. Moreover, for $N \to \infty$ it can be assumed that $C_A/C_F \ll N$. Thus, the loss of the conformational entropy due to the terminal chain attachment can be calculated as follows:[62]

$$\frac{\Delta S}{k_B} = \frac{1}{k_B} \ln\left(\frac{\Omega_F}{\Omega_A}\right) = (\gamma_F - \gamma_A) \ln N \tag{2}$$

where $k_B$ is the Boltzmann constant. Equation 2 suggests that $\Delta S$ is a linear function of $\ln(N)$ and is independent of any other system parameters. Although this equation was obtained for $N \to \infty$, the rectilinear dependence of $\Delta S$ on $\ln(N)$ was found numerically for chains of length $N$ from 1 to 50 monomer units that were terminally attached to the infinite plane.[62]

The calculations of the reduction of the conformational entropy of a polymer chain caused by a particle inserted into the coil domain can be also performed using the scaling theory.[64−66] If a particle of diameter $D$ is introduced into the coil, the probability $p$ of its interacting with the polymer or—in other words—the fraction of the coil volume denied to the particle is

$$p \sim \left(\frac{D}{R_G}\right)^{4/3} \tag{3}$$

where $R_G$ is the radius of gyration of the polymer coil. The loss of conformational entropy due to the insertion of a particle can be calculated as follows:

$$\frac{\Delta S}{k_B} = -K(L)\left(\frac{D}{N^{\nu}}\right)^{4/3} \tag{4}$$

where $K(L)$ is a constant dependent on the segment length, $L$, and $\nu$ is the scaling exponent in the relation $R_G \sim N^{\nu}$ equal to ${}^3/_5$.[67]

The value of $\Delta S$ calculated on the basis of eq 4 is independent of the shape of the particle and its location in the coil domain, but it depends on the particle diameter, $D$, and the chain length. For a fixed $D$, the shorter the chain the larger the entropy loss, and as $N$ grows, the entropy loss goes to zero. As $D$ grows, the entropy loss increases since more space is excluded by the particle.

The above-presented methods of calculation of the conformation entropy of the polymer chain in the presence of a colloidal particle are subject to certain limitations. For instance, eq 2 has been derived for extremely long chains, but it has been verified only for relatively short chains attached to a plane, while in eq 4 the distribution of the segment density in the polymer coil is not taken into account.

## 2. Methods

In this study the effect of small colloidal particles on the structure of polymer coil and the coil conformational entropy is considered by means of the SAW chain on the 3D cubic lattice. Two cases are examined: the insertion of nonadsorbing particle into the coil domain and the irreversible attachment of one chain end to the particle.

The study was performed assuming several major approximations: (i) only the diluted athermal polymer solution is considered, (ii) the solution is modeled by a cubic lattice (the configurational properties of the chain do not depend on the structural details of the lattice except its dimensionality), and (iii) the limit of linear, long, and flexible polymer chains, modeled by the SAW chains, and colloidal particles small when compared with the size of the macromolecules is taken.

In the study, several numerical methods were applied:

**2.1. The Rosenbluth MC Method.**[68] The method is based on step-by-step generation of the SAW chains accompanied by the calculation of transition probabilities defined in 3D cubic lattice as the ratio $p_i = n_i/5$, where $n_i$ is the number of the lattice cells surrounding a currently generated segment, which are not occupied by another segment. Then the Rosenbluth−Rosenbluth weighting factors, $b_i(N)$, were calculated for each polymer chain from eq 5:[68]

$$b_i(N) = \prod_{i=1}^{N} p_i \tag{5}$$

Considering the difference between computational and thermodynamical possibilities, the mean value of a parameter describing the coil properties was calculated as follows:[68]

$$\bar{x}(N) = \frac{\sum_{k=1}^{m} b_k(N)\, x_k(N)}{\sum_{k=1}^{m} b_k(N)} \tag{6}$$

where $m$ is the number of conformations (equal to $10^6$ for all considered chain lengths) and $x$ means the parameter value.

**2.2. The Statistical Counting Method (SCM).**[52] The SCM was used to calculate the conformational entropy of long chains. The method is based on the calculation of the quantity defined as

$$\omega_i = \frac{\Omega_{i+1}}{\Omega_i} \tag{7}$$

where $\Omega_i$ is the number of conformations of a chain of $i$ segments. The physical meaning of $\omega_i$ can be related to the effective coordination number of the lattice (it is equal to 5 for the first three segments, then $\omega_i \leq 5$). If $\omega_i$ values are known, the total number of conformations of the chain built of $N$ segments can be calculated as

$$\Omega_N = \prod_{i=1}^{N-1} \omega_i \tag{8}$$

The effective coordination numbers were obtained on generation of SAW chain conformations. The data set generated consisted of $m = 10^6$ different conformations of a chain of 2200 segments. We have collected also data for shorter chains (with a step of 100 segments). The number of shorter chains was greater than $m$, because the SCM allows us to take into account the information from dead chains.[52] In our study, instead of $\omega_i$, the average $\bar{\omega}_i$ values obtained by the MC sampling method were used. In the calculations of $\bar{\omega}_i$, the Rosenbluth–Rosenbluth weighting factor (eqs 5 and 6, $x = \omega_i$) was considered. The entropy of the chain was calculated from the equation

$$\frac{S_N}{k_B} = \sum_{i=1}^{N-1} \ln(\bar{\omega}_i) \tag{9}$$

To calibrate our simulations, the dependence of $R_G$ of free polymer chains on $N$ was examined. As expected for SAW chains in the cubic lattice,[69] we obtained $R_G \sim N^{2\nu}$ with $\nu$ equal to $0.58 \pm 0.02$. Moreover, the results of SCM were confronted with those obtained by means of the direct counting method (DCM) and RG theory (eq 1) in the way described in ref 52.

Prior to the coil generation, an impenetrable object was placed in the lattice. Two types of objects were considered: cubelike particles of different volumes and some infinite obstacles like plane, half-infinite plane, line, and needle. The coil generation was initiated at the lattice cell next to the object. The attachment point was chosen exactly at the center of the particle wall in the case of odd edge lengths or near the center in other cases. The segment density distribution, the average radius of gyration, $R_G$, the end-to-end distance, $\langle R^2\rangle^{1/2}$, and the distance between the mass center of the coil and the attachment point (or, in the case of free coil, the distance between the coil mass center and the chain end), $Z$, were calculated simultaneously during the simulations.

**2.3. Analysis of the Cavity and Adsorption Site Distributions in the Polymer Coil.** The distributions of empty regions in the coil, further named as cavities, of different volumes were determined for unperturbed coils and the coils distorted by the irreversible particle adsorption. Analysis of the structure of an unperturbed coiled chain consisted of two stages: generation of a SAW coil of a length $N = 1000$ by means of the Rosenbluth MC method[68] in the 3D cubic lattice and the search for cavities in the "frozen" coil. In the second stage, a cubic particle of a volume $V$ was moving in the coil domain in such a way that the particle center was successively shifted from one cell to another. After each step, the area occupied by the probing particle was examined for the presence of (i) lattice cells occupied by polymer segments and (ii) cells neighboring the segment-occupied ones. On the basis of the results obtained, the following distributions were constructed: (i) the cavity distribution, which informs about all possible positions of the particle of volume $V$ in the coil domain; (ii) the adsorption site distribution, which is the distribution of possible positions of the particle of volume $V$, in which the particle occupies at least one cell adjacent to the segment-occupied cell.

The structure of a coil distorted by the irreversible particle attachment was examined in a way similar to that of analysis of the structure of the unperturbed chain. At first, the SAW coil of a length $N = 1000$ was generated. Then, the processes of particle adsorption and chain reconformation were simulated. After a conformation sample of a chain had been generated, a particle of a volume $V$ was placed in a cavity. The cavity of a volume large enough to accommodate the particle and situated nearby the mass center of the coil was chosen. Then, the polymer coil was relaxed. The relaxation process was simulated by random elementary modifications of the chain, such as trans–gauche and gauche–trans moves of the chain ends and kink-jump or crankshaft moves of other segments,[71–73] based on the simplified Metropolis MC method.[70] The simplification of the method was the acceptance of all segment shifts (which is equivalent to the assumption of athermal system) except those of segments located in the cell adjacent to the particle position, which were assumed to be adsorbed irreversibly and were not moved any more. To establish the simulation length sufficient for reaching the equilibrium chain conformation, we check simulation lengths equal to $10^7$ and $5 \times 10^7$ trial moves per conformation. We found that additional moves did not cause any systematic changes in the cavity distributions; hence, we accepted the simulation length equal to $10^7$ trials. After the equilibration had been reached, the conformation was "frozen" and searched for cavities. The volume of the probing particle was always equal to the volume of the adsorbed one.

The average distributions of cavities and adsorption sites were calculated with Rosenbluth–Rosenbluth weighting factors (eqs 5 and 6, $x$ means the cavity density) for an ensemble of $10^4$ chain conformations.

## 3. Results and Discussion

**3.1. Free Particle in a Polymer Coil.** The radial distribution of the number of segments around the mass center of the coil modeled by the normal random walk (NRW) (no volume excluded by polymer chain applied) is given by eq 10:[74]

$$W_N(R) = \frac{108 R_d^{\,2}}{\sqrt{\pi N L^3}} \exp\left(-\frac{9 R_d^{\,2}}{N L^2}\right) \tag{10}$$

or

$$W_N(r) = \frac{108 r^2}{\sqrt{\pi N L}} \exp\left(-\frac{9 r^2}{N}\right) \tag{10a}$$

where $R_d$ is the distance of a lattice cell from the mass center of the coil and $r$ is the relative distance from the center equal to $R_d/L$.

To calculate the radial segment distribution of chains with excluded-volume interactions, we used Rosenbluth–MC method. The results obtained for the generated conformations, together with the distribution obtained for NRW chains (without excluded-volume interactions), are presented in Figure 1. The two distributions are practically identical provided that the space coordinates are rescaled using the simple power law ($r^2 \rightarrow r^{1/\nu}$). Thus, the radial segment distribution

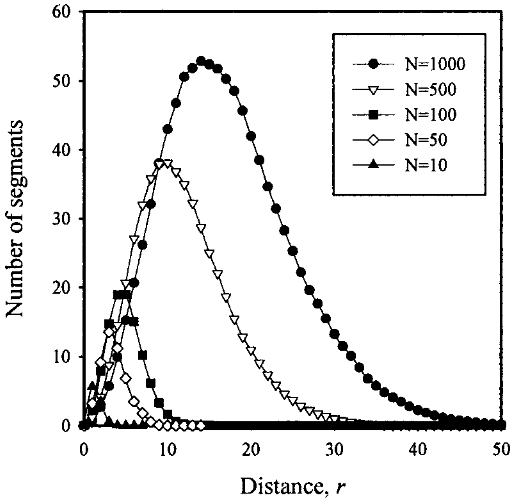

**Figure 1.** Segment distributions around the mass center of the coil for different chain lengths (points, results of the simulation; curves, calculated from eq 10).

around the center of the SAW coil can be expressed by eq 11:

$$W_N(r) = \frac{72r^{1/\nu}}{\sqrt{\pi N L}} \exp\left(-\frac{9r^{1/\nu}}{N}\right) \tag{11}$$

where $\nu = 0.58 \pm 0.02$ for the cubic lattice. The $\nu$ value was obtained by the fit of calculated SAW distributions to eq 11.

By differentiating eq 11, we get

$$R_m = \left(\frac{L\sqrt{N}}{3}\right)^{2\nu} \tag{12}$$

where $R_m$ is the distance from the mass center of the coil, corresponding to the highest probability of finding a segment.

Assuming that all linear coil parameters scale with the same exponents,[53] the radius of gyration, $R_G$, and the root-mean-square end-to-end distance, $\langle R^2\rangle^{1/2}$, can be defined by

$$R_G = \left(\frac{L\sqrt{N}}{\sqrt{6}}\right)^{2\nu} \tag{13}$$

$$\langle R^2\rangle^{1/2} = (L\sqrt{N})^{2\nu} \tag{14}$$

The obtained value $\nu$ is close to that obtained by testing eqs 13 and 14 on the cubic lattice ($\nu = 0.58 \pm 0.02$) or the one resulting from RW theory ($\nu = {}^3/_5$).[69]

On the basis of eq 11, the segment density distribution in a polymer coil can be found:

$$W(r) = \frac{18}{\sqrt{\pi^3 N L}} \exp\left(-\frac{9r^{1/\nu}}{N}\right) \tag{15}$$

The distribution (15) gives the probability that a polymer conformation passes through a lattice cell which is at a distance $r$ from the coil center. Thus, the product $\Omega_F W(r)$ gives the number of all conformations that pass through this cell.

If a colloidal particle of a volume equal to the lattice cell volume is placed in the domain of the coil, a number of coil conformations are eliminated from the total number of conformations $\Omega_F$. Taking into account that each SAW conformation can pass through the lattice cell only once, $\Omega_F W(r)$ yields the number of conformations eliminated. Thus, when the particle is shifted from the bulk to the coil domain, the entropy loss due to the increase in the excluded volume can be expressed as

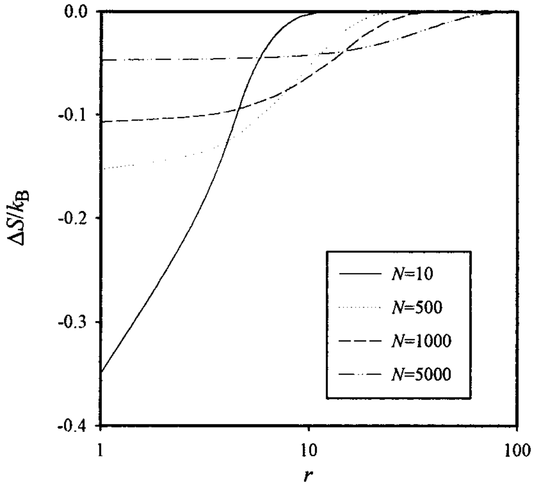

**Figure 2.** Entropy reduction as a function of the particle position in the polymer coil.

$$\frac{\Delta S(r)}{k_B} = \ln(\Omega_F - \Omega_F W(r)) - \ln(\Omega_F) = \ln\left(1 - \frac{18}{\sqrt{\pi^3 N L}} \exp\left(-\frac{9r^{1/\nu}}{N}\right)\right) \tag{16}$$

For very long chains eq 16 can be rewritten in a simpler form:

$$\frac{\Delta S(r)}{k_B} = -\frac{18}{\sqrt{\pi^3 N L}} \exp\left(-\frac{9r^{1/\nu}}{N}\right) \tag{16a}$$

The dependence of $\Delta S$ on the particle location in the coil domain, calculated from eq 16, is shown in Figure 2. With increasing chain length, the shape of the curve flattens. In the case of very long chains, introduction of a particle into the central part of the coil causes only small changes in $\Delta S$.

Equation 16 gives the entropy loss induced by a very small particle of a diameter equal to the segment length only. Nonetheless, it can be applied when the statistical length of the polymer segment is comparable with the particle radius. The size of the physical segment is not just the size of the chemical monomer, but rather of a group of successive chemical monomers whose size is of the order of the Kuhn length[75] over which the directional correlation between the chemical units disappears. For example, the Kuhn parameter of polyacrylamide is equal to 15,[76] which gives the statistical segment length of 5 nm. This length is comparable with diameters of typical micelles or protein globules.

If a larger particle is considered, a greater number of chain conformations are eliminated, because the particle occupies more than one lattice cell. However, since there are chain conformations simultaneously passing through two or more cells occupied by the particle, the number of conformations eliminated increases less strongly than the particle volume. To consider this effect, let us introduce the number of local conformations of the polymer chain, $w$, which represents a number of possible conformations of a chain section which pass through the

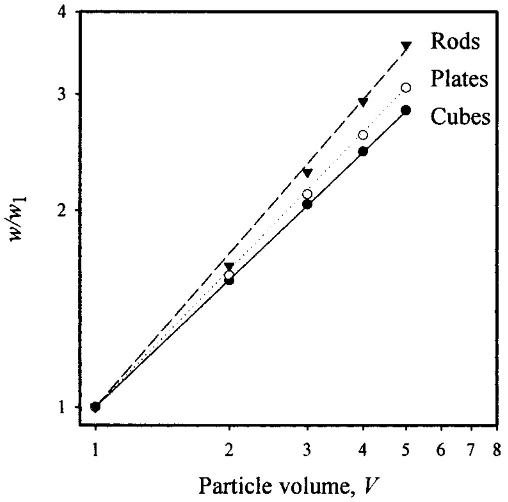

**Figure 3.** Relation between $w/w_1$ and the volume of the particle.

**Table 1. Values of Exponents of Eq 12**

| particle shape | $s$ |
|---|---|
| rod | $0.78 \pm 0.02$ |
| plate | $0.69 \pm 0.02$ |
| cube | $0.65 \pm 0.02$ |

volume occupied by a particle. In the cubic lattice, there are $w_1 = 15$ possible local conformations passing through one cell. (There are 15 different ways to link two centers of cube walls by a chain section.) When calculating the local conformation number for two adjacent cells, five local conformations crossing the wall between two neighboring cells and a number of those that cross other walls of both cells simultaneously should be subtracted from the number of $2w_1$ conformations. This case corresponds to the loop formation. The number of loops decreases very fast with their increasing lengths. For example, the contribution of different loops to the total number of local conformations was calculated as a series of $1/5^i$ ratios, where $i$ is the loop length.

The dependencies between the relative number of local conformations, $w/w_1$, and the particle volume, $V$, for particles of different shapes are shown in Figure 3. As seen, the more compact the shape, the smaller the $w/w_1$ ratio. The relation $w/w_1 = f(\ln(V))$ is linear, and its slope depends on the particle shape. Thus, it can be written

$$\frac{w}{w_1} = V^s \tag{17}$$

The values of $s$ calculated for different shapes of particles are collected in Table 1.

Equations 16 and 17 can be used for the calculation of the entropy changes caused by a particle larger than the lattice cell, provided that the segment distribution in the space occupied by the particle is uniform. Such a uniformity can be assumed in the case of small particles inserted into large coils, except the coil peripheries.

The extent of reduction of the macromolecule conformational entropy, due to the introduction of a small particle into the coil, depends on the particle shape and position in the coil domain. For infinite chains, the entropy drops to zero. The entropy reduction leads to the entropy driven removal of the particle from the coil.

### 3.2. The Chain with One End Attached to a Particle.

To find the number of conformations of a chain with one end attached to a particle, we have applied two methods: DCM and SCM.[52] DCM takes a lot of CPU time so we used it only for analysis of very short chains.

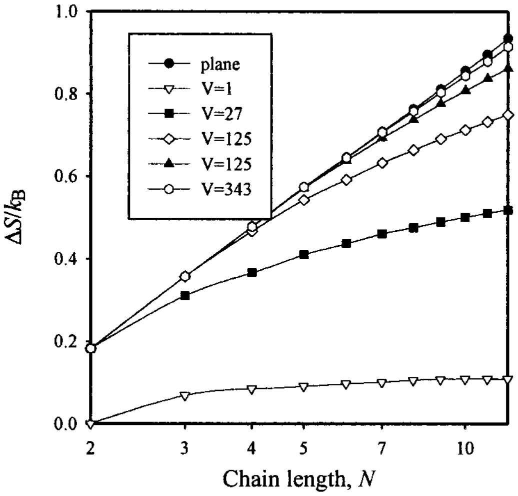

**Figure 4.** Differences in the entropies of free and terminally attached chains vs the chain length. Cubic objects of different volumes and the plane are considered. The number of conformations was calculated by means of DCM.

Figure 4 shows the results obtained with DCM. The entropy reduction caused by attachment of the terminal segment to an impenetrable surface is plotted against the chain length. Different types of objects were considered: cubelike particles of various volumes and the infinite plane. From a linear dependence $\Delta S = f(\ln(N))$, found for the plane-attached chains, a simple power law results:

$$\frac{\Delta S}{k_B} = \ln\left(\frac{\Omega_F}{\Omega_A}\right) = \beta \ln(N) \tag{18}$$

where $\beta = 0.42 \pm 0.01$.

Equation 18 takes the form predicted by the RG theory (for the sake of comparison see eq 2) and confirmed by the calculation with the DCM and the MC method.[62] However, as seen in Figure 4, the $\Delta S$ values found for the particle-attached chains differ from those calculated from eq 18. The smaller was the particle the more distinct was the difference. The curves calculated for particle-attached chains seem to tend to a certain limit. However, in the range of polymer lengths analyzed by the DCM, these limiting values were not obtained.

To calculate the conformational entropy of long chains, the SCM was used. The results of simulations are collected in Figures 5−13. The averaging of the all coil parameters was performed using the Rosenbluth−Rosenbluth weighting factors (eqs 5 and 6).

Figures 5 and 6 present the effect of the particle volume on the radial segment distribution around the mass center of the coil and around the attachment point, respectively. Since the distributions obtained for the terminally attached and free chains do not differ very much, for better illustration of the effect Figures 5 and 6 show the differences between these distributions; for the sake of comparison, the distribution for the free chain is also included.

As follows from Figure 5, the chain attachment results in a reduction of the height of the maximum and an increase of the number of segments present near the

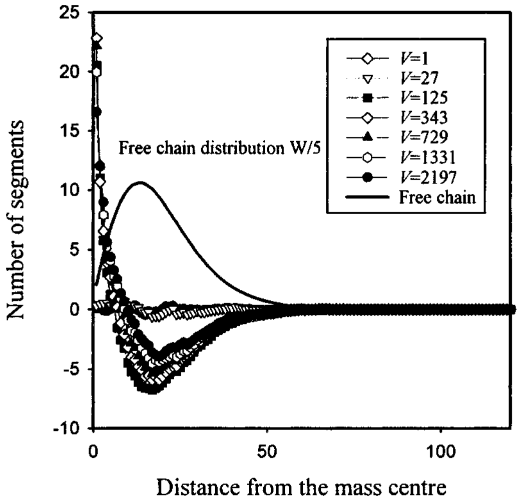

**Figure 5.** Effect of terminal chain attachment on the radial segment distribution around the chain mass center: difference between the distributions of free and particle-attached chains. Particles of different volumes are considered. For the sake of comparison, the distribution of free chain, scaled down in 1:5 ratio, is presented.

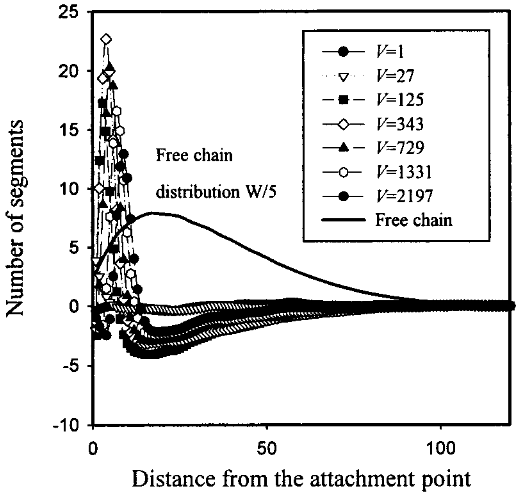

**Figure 6.** Effect of terminal chain attachment on the radial segment distribution around the attached end of the chain: difference between the distributions of free and particle-attached chains. Particles of different volumes are considered. The distribution of free chain, scaled down in 1:5 ratio, is shown.

mass center. Such changes in the segment distributions point to the coil contraction. The larger the particle the more distinct the difference between the shapes of the attached and free chains.

From the results presented in Figure 6, a weak coil contraction induced by the chain attachment can be also concluded, since the number of segments occurring near the chain end increases after its attachment. On the distribution curves sharp maxima appear, whose positions correspond to the distances of attachment points from the nearest edges.

The segment distributions found for the chains attached to infinite objects do not differ very much from those obtained for particle-attached chains; the largest perturbations are found for plane-attached chains. This phenomenon can be explained by the fact that, from among the objects examined, the plane eliminates the greatest number of conformations.

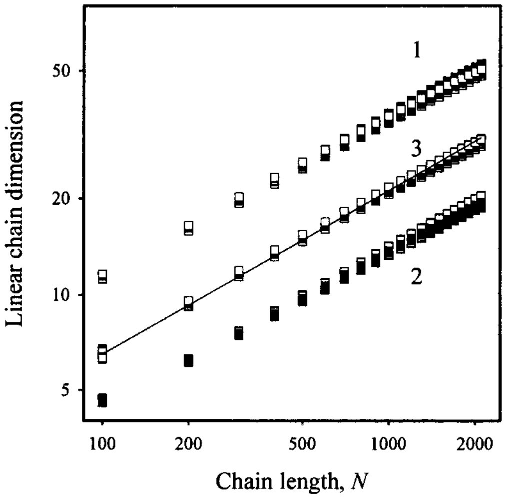

**Figure 7.** Effect of the chain length on $\langle R^2\rangle^{1/2}$ (1), $R_G$ (2), and $Z$ (3) values. The calculations were performed for free and particle-attached chains; particles of different volumes are considered ($V = 1$, 27, 125, 343, 1331, and 2197).

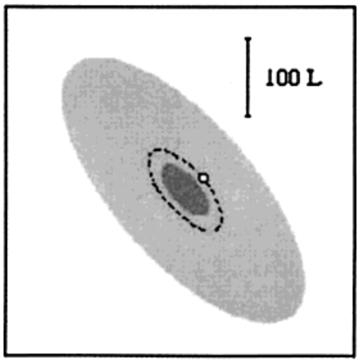

**Figure 8.** Ellipsoid whose dimensions are determined by the average separation of the most distant segments of a long chain terminally attached to a small particle. The most probable particle position is marked by the dashed line. The size of the dark area is determined by $R_G$.

Figure 7 illustrates the effect of the length of terminally attached chains on the three linear dimensions: $\langle R^2\rangle^{1/2}$, $R_G$, and $Z$. The dependencies resemble those for free chains and can be described by the same power laws. The values of $Z$ are equal to the geometrical average of the end-to-end distance and the radius of gyration, irrespective of the particle radius:

$$Z = \sqrt{\langle R^2\rangle^{1/2} R_G} = \left(\frac{L^2}{\sqrt{6}} N\right)^{\nu} \qquad (19)$$

In Figure 8, a very long polymer chain, terminally attached to a small particle, is schematically represented as an ellipsoid, whose dimensions correspond to the average separation of the most distant segments. The mean radius of the dark part of the ellipsoid is equal to $R_G$. The dashed line marks the most probable separation of the particle from the mass center of the coil, $Z$. As follows from Figure 7, $Z$ is always higher than $R_G$, which indicates the entropy driven tendency to push an object out of the coil interior.

The exponents $\nu_F$ and $\nu_A$ of eqs 13, 14, and 19 were found by fitting the straight lines to the dependencies shown in Figure 7. The ratios of $\nu_A/\nu_F$, obtained for different $V$ values, are presented in Figure 9. Only a slight effect of $V$ on $\nu_A$ is observed (the deviations of

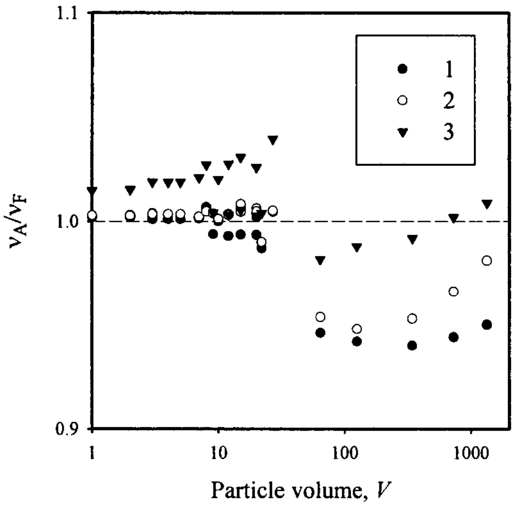

**Figure 9.** Relation between $\nu_A/\nu_F$ and the particle volume (1 − $\langle R^2\rangle^{1/2}$, 2 − $R_G$, and 3 − $Z$).

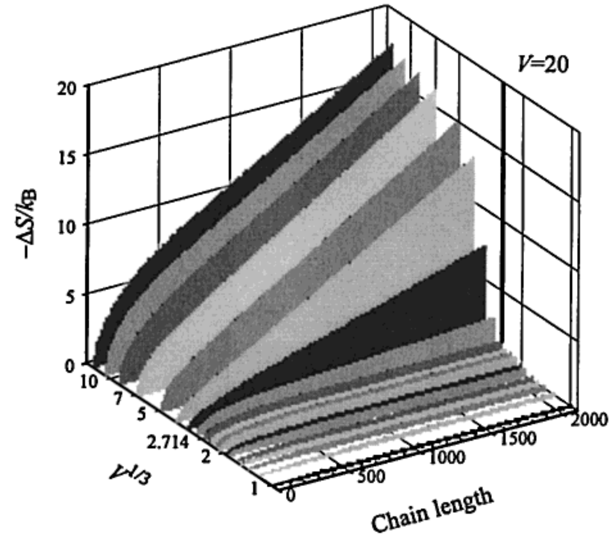

**Figure 10.** Effect of chain length on the entropy loss caused by the terminal chain attachment to particles of different volumes.

$\nu_A/\nu_F$ do not exceed 0.006). A certain scattering of the results should be ascribed to the fact that different shapes of particles and different positions of the chain-attachment points at the particle surface were considered. In Figure 9, two regions can be distinguished: (i) for $V \leq 20$, where the particle−polymer attachment practically does not affect the chain dimensions, and (ii) for $V > 20$, where the coil contraction due to the particle binding takes place.

Figure 10 presents the effect of the chain length on the reduction of the conformational entropy of macromolecule caused by the attachment of one chain end to the particle surface. Particles of different volumes were considered. In the case of short chains ($N < 500$), the higher $N$ the greater $\Delta S$, irrespective of the particle volume. For longer chains ($500 < N < 2200$) the character of the relationship $\Delta S = f(N)$ depends on $V$. And thus, for $V \leq 20$, $\Delta S$ values tend to a certain limit $\Delta S_{\max}$, whereas if $V > 20$ a rectilinear increase of $\Delta S$ with increasing chain length is observed.

For particles of $V > 100$ and for chains of length $N$ from 500 to 2200 (see Figure 10), we obtain by fitting

$$\Delta S = AD + BN \tag{20}$$

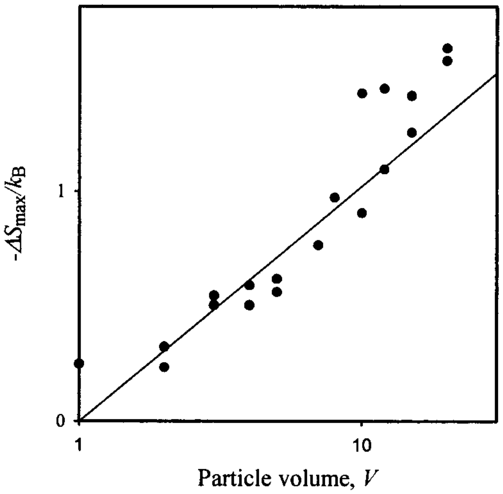

**Figure 11.** $\Delta S_{\max}$ vs particle volume for $V \leq 20$.

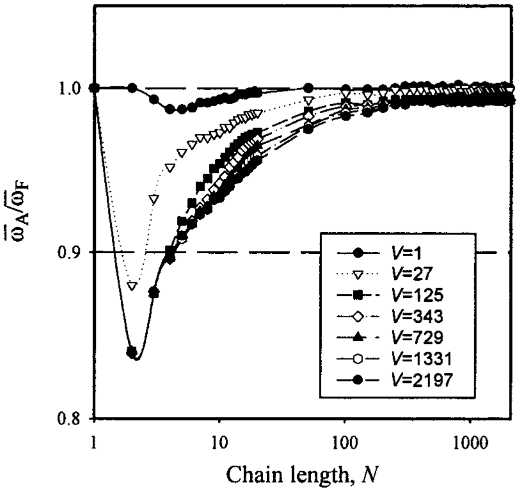

**Figure 12.** Relations between the relative coordination number $\bar{\omega}_A/\bar{\omega}_F$ and chain length, $N$, obtained for different particle volumes.

where $A$ and $B$ are constants and $D$ is an average length of particle edge ($\sqrt[3]{V}$).

In the case of chains attached to particles of $V \leq 20$, there is a rectilinear dependence of $\Delta S_{\max}$ on ln($V$), as shown in Figure 11. The scattering of points can be ascribed to different shapes of particles considered. The fit of a straight line to the points obtained from the simulations leads to

$$\Delta S_{\max} = -Ak_B \ln V \tag{21}$$

where $A = 0.50 \pm 0.02$.

The effect of the chain length on $\Delta S$ can be explained by analysis of variation of the effective coordination number of the lattice, $\bar{\omega}$, with $N$. In Figure 12, the dependencies of the relative coordination number (i.e., the ratio of the coordination number of attached and free chains, $\bar{\omega}_A/\bar{\omega}_F$) on the chain length, obtained for different $V$ values, are shown. For short chains, $\bar{\omega}_A$ values are small as compared with those of $\bar{\omega}_F$, whereas in the case of long chains $\bar{\omega}_A$ values reach a certain limit; if $V \leq 20$ the limit is equal to $\bar{\omega}_F$, whereas for $V > 20$ it is somewhat smaller than $\bar{\omega}_F$. The obtained relations between $\bar{\omega}_A$ and $N$ are intuitively obvious: the shorter the chain the higher the probability of finding the free end near the particle surface.

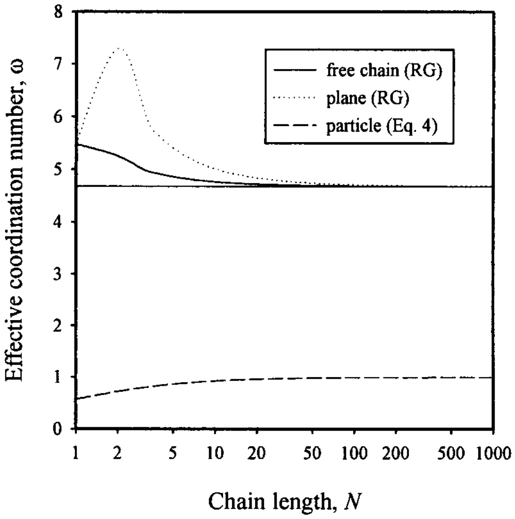

**Figure 13.** Dependence of the effective coordination number, $\omega$, on the chain length, calculated for the free chain (eq 1), the chain terminally attached to the plane (eq 2), and the polymer coil with a colloidal particle inside (eq 4).

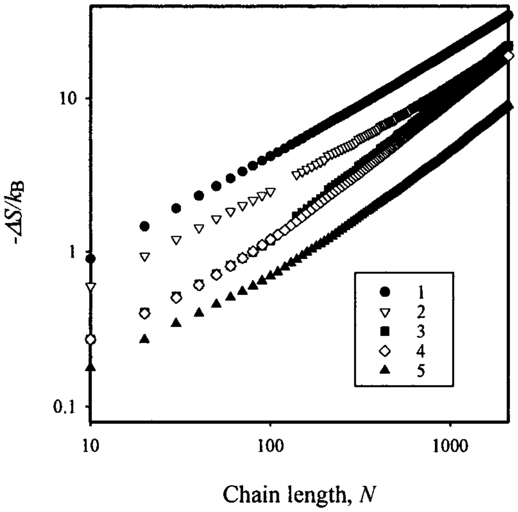

**Figure 14.** Influence of the chain length on the entropy loss due to the terminal chain attachment to various infinite objects (1, plane; 2, 3, edge of half-infinite plane; 4, line; 5, end of the needle; in the case of half-infinite-plane-attached chains, two different orientations of the first segment are considered.)

For the sake of comparison, dependencies of $\omega$ on $N$ were also determined on the basis of the RG (eqs 1 and 2) and scaling (eq 4) theories. The obtained results are shown in Figure 13. As follows, for short chains the RG theory predicts $\omega$ values higher than the possible maximum effective coordination number of the cubic lattice (which is equal to 5) and suggests $\omega_A > \omega_F$. Thus, the RG theory fails for short chains (although eq 2 describes correctly the dependence of $\Delta S$ on $N$). On the other hand, the relation obtained on the basis of eq 4 describes correctly the effect of $N$ on $\omega_A$ values; however, it does not predict the dependence of $\omega_A$ on the particle volume, found by means of SCM.

The relations between $\Delta S$ and $N$, calculated for the chains attached to infinite objects, are presented in Figure 14. For plane-attached chains, a rectilinear dependence of $\ln(\Delta S)$ on $\ln(N)$ was obtained, unlike the one found by means of DCM for $N \leq 12$ (Figure 4). This discrepancy suggests that eq 2, based on the RG theory, is valid for short chains only. The dependencies $\Delta S = f(N)$ found for other infinite objects (half-infinite plane, line, needle) are more complex than that obtained for the plane.

The results of the studies of the effect of terminal chain attachment to different objects on the conformational entropy of macromolecules are summarized in Table 2. It also includes the equations for the entropy calculations found by the numerical analysis of the simulation results presented in this section.

In summary, we can say that the entropy loss due to the terminal attachment of very long flexible chains to small colloidal particles depends on the particle size and the chain length. However, in the case of extremely small particles, $\Delta S$ does not depend on the chain length, but only on the particle size, which implies that such particles induce only a local coil perturbation. There is the entropy-driven tendency to locate the particle in the peripheries of the coil.

**3.3. Energy of Adsorption.** Reversible polymer adsorption takes place when the energy of adsorption exceeds the entropy loss associated with the reduction in the number of conformations available to the chain. Thus, the knowledge of the entropy changes—accompanying the chain attachment to a particle—allows evaluation of the minimum value of energy necessary for the adsorption to occur.

If the particle is small and the polymer molecule is very large, it can be assumed that the entropy reduction is practically independent of the particle position along the chain, since only a local disturbance of the segment density distribution is expected. Thus, eq 20, which gives the entropy loss due to terminal chain attachment, can be used for calculation of the entropy reduction caused by attachment of a particle to any site along the chain. The adsorbing particle can create a number of contacts with the polymer chain. An adsorption layer, which consists of a number of chain loops, is formed. Therefore, in the case of adsorption, one should take into account that the particle radius is enlarged by the adlayer thickness and that the free section of the chain is shortened.

To calculate $\Delta S$ values, we assumed that the thickness of the polymer adlayer is equal to the particle radius[26] (see also the section 3.4) and the adlayer's entropy is negligibly small as compared with the entropy of the free section of the chain. Moreover, two values of the segment density in the adsorption layer, $d$, were arbitrarily chosen. We selected $d$ values close to the extreme ones in order to avoid their calculation as they are complex functions of many parameters like, for instance, the energy of monomer adsorption, the statistical segment length, or the particle radius. On the basis of the obtained $\Delta S$ values, the minimum adsorption energy per the surface unit of the particle, $\Delta E_{\min}$, needed to outweigh the conformational entropy effect, was evaluated.

The influence of the particle size and the chain length on $\Delta E_{\min}$, examined at two different segment densities in the adsorption layer, is summarized in Figure 15. As seen, the shape of the relation depends on the assumed $d$ value. For low $d$, $\Delta E_{\min}$ decreases with increasing $V$; for high $d$, the curves go through a minimum. The complex character of these dependencies can be understood taking into regard the influence of the particle size on the free energy of adsorption related to two opposite effects. One of them is an increase in the number of

**Table 2. Effect of the Terminal Chain Attachment on the Conformational Entropy**

| object | $\Delta S = f(N)$ | $\Delta S$ | $S_A$ |
|---|---|---|---|
| particles ($V \le 20$) | 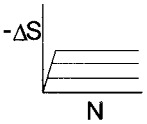 | $\Delta S/k_B = \ln(C_F/C_A)$<br>$C_A = f(V/L^3)$ | $S_A/k_B = \ln(C_A) + (\gamma_F - 1)\ln N + N\ln(\mu_F)$<br>$C_A = C_F V^{-A_1} = C_F D^{-3A_1}$<br>$A_1 = 0.50 \pm 0.02$ |
| particles ($V > 100$) | 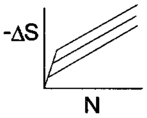 | $\Delta S/k_B = \ln(C_F/C_A) + N\ln(\mu_F/\mu_A)$<br>$C_A = f(D/L)$,<br>$\mu_A = \text{const} \neq \mu_F$ | $S_A/k_B = \ln(C_A N^{\gamma_F - 1}\mu_A{}^N)$<br>$C_A = C_F \exp(-A_1 D)$<br>$\mu_A = A_2\mu_F$<br>$A_1 = 0.27 \pm 0.02$; $A_2 = 0.994 \pm 0.002$ |
| plane (short chains, DCM) | 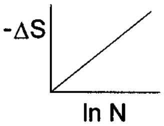 | $\Delta S/k_B = (\gamma_F - \gamma_A)\ln N$<br>$\gamma_A \neq \gamma_F$ | $S_A/k_B = \ln(C_F N^{\gamma_A - 1}\mu_F{}^N)$<br>$\gamma_A = \gamma_F - A_1$<br>$\gamma_A = 0.75 \pm 0.01$<br>$A_1 = 0.42 \pm 0.01$ |
| plane (long chains, SCM) | 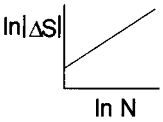 | $\Delta S/k_B = AN^{\alpha}$ | $S_A/k_B = \ln(C_F N^{\gamma_F - 1}\mu_F{}^N) - AN^{\alpha}$<br>$\alpha = 0.69 \pm 0.01$<br>$A = 0.17 \pm 0.01$ |

polymer–particle contacts upon increasing $V$ (and the particle surface as well). The higher the number of contacts the higher the total adsorption energy and hence the lower $\Delta E_{\min}$ needed to outweigh the entropy loss. At the same time, however, the increase in $V$ brings about the opposite effect on the free energy of adsorption; that is, it implies a greater reduction in the chain conformational entropy. The extent of the reduction depends on $d$; the higher $d$ the higher $\Delta S$ due to the greater number of segments involved in the adlayer formation. Above a certain particle volume, if a dense adlayer is formed, the entropic effect seems to increase faster with the particle size than the energetic one, connected with the increased number of polymer–particle contacts.

In the range of very small $V$, irrespective of $d$, $\Delta E_{\min}$ assumes relatively high values, and it increases with decreasing $V$. Von Goeler and Muthukumar[9] have even predicted the existence of a critical particle radius, below which the polyelectrolyte adsorption does not occur. The obtained dependence of $\Delta E_{\min}$ on the particle size is also in accordance with the results of studies on the kinetics of adsorption of nanosized gold particles on very-high-molecular weight polyacrylamide;[77] larger particles were found to adsorb faster.

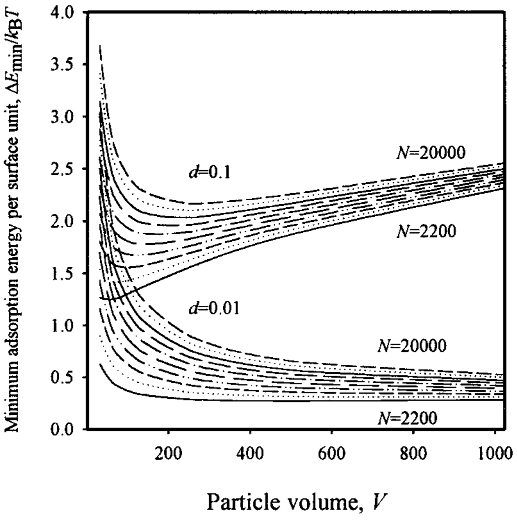

**Figure 15.** Dependence of $\Delta E_{\min}$ on the particle volume; different chain lengths, $N$, and segment densities in the adsorption layer, $d$, are considered.

The length of the chain also affects $\Delta E_{\min}$. As follows from Figure 15, the increase in $N$ involves a certain, but not great, increase in $\Delta E_{\min}$. An explanation is that the longer the chain the greater the contribution of the loss in conformational entropy to the free energy of adsorption (see Figure 10). Such an explanation was already assumed for the elucidation of the preferential adsorption of low-molecular-weight polymers on small objects.[33]

**3.4. Diffusion and Adsorption of a Particle in Polymer Coil.** In the adsorption process three main steps can be distinguished: the diffusion of the particle to a place of encounter with the macromolecular strand, the particle attachment, and the polymer reconformation associated with the free energy minimization. A small particle can enter a large polymer coil. The depth to which it can enter the coil, before the polymer strand encounter, depends on the particle size and the coil conformation.

The polymer coil is a dynamic structure, which means that the local densities of segments and cavities in the coil are time-dependent. Although the cavities are only temporary species, the knowledge of their distributions can give insight into the diffusion of the particle through the coil. The distribution of empty lattice cells in the coil domain can be calculated easily from eq 11. However, the calculation of distribution of cavities of a given volume is nontrivial.

To solve the problem, we performed a statistical analysis of the cavity distribution in the polymer chain. The results of the simulations are collected in Figures 16–19.

As follows from the cavity distributions presented in Figure 16, the unperturbed chain can be easily penetrated by extremely small particles, since the density of cavities of $V = 1$ is quite high even in the coil interior. There is only a small minimum, whose depth does not exceed 15% of the maximum cavity density. With increasing volume of cavities the depth of the minimum increases, indicating that the coil penetrability by the particles decreases with increasing particle size. A

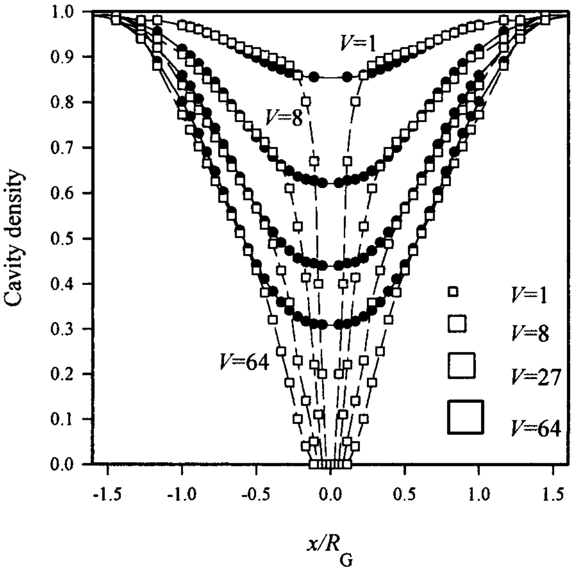

**Figure 16.** Density of cavities vs the relative distance from the coil center, $x/R_G$ (solid lines, free chain; dashed lines, adsorbed chain, $N = 1000$; cavities of volumes equal to 1, 8, 27, and 64 are considered).

reduction of the cavity density occurs practically in the area limited by $R_G$ only.

In the space occupied by the adsorbed particle the cavity density is equal to zero. Therefore, the deep minima observed on the cavity density distributions of adsorbed chains can be ascribed to the presence of particles. The widths of the minima exceed, however, the edge lengths of the particles attached. The larger widths of the minima as compared with the edge lengths can be ascribed to the presence of adsorbed polymer layers on particle surfaces. The fact that the width of a minimum changes gradually with the changing distance from the particle surface points to the absence of a well-marked boundary between the adlayer and the rest of the coil. This, in turn, evidences the presence of adsorbed loops of different lengths. The width of each minimum, measured in the middle of its depth, is approximately 3 times as large as the particle edge, $D$. It means that the smallest possible distance between the centers of attached and probing particles is $^3/_2D$. On the basis of this value an average thickness of an adsorbed layer can be evaluated as $D/2$. This result is in accordance with recently reported results of Aubouy and Raphaël,[26] who studied the adsorption of a long chain on a small particle by means of the scaling theory and found the adsorption layer to be composed of only short loops comparable in size to the particle radius. Similar results were obtained by Marques and Joanny.[19]

Figure 17 presents the probability $p_k$ that a particle of volume $V$ will find its way toward the coil center, with no collision with a chain segment. The probability was calculated on the basis of cavity density distribution:

$$p_k = \prod_{i=\infty}^{k} \rho_i \tag{22}$$

where $\rho_i$ denotes the cavity density.

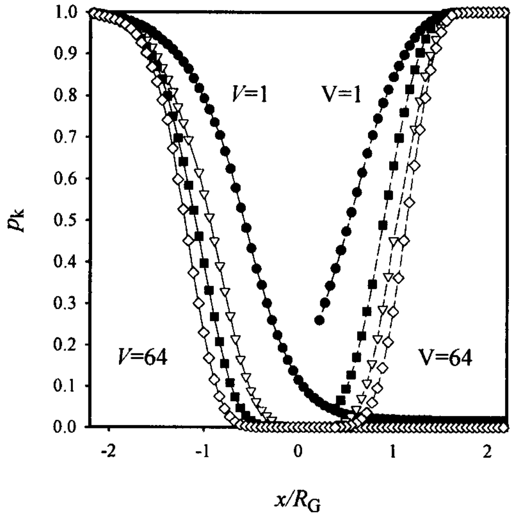

**Figure 17.** Probability of coil penetration, $p_k$, vs the relative distance from the coil center, $x/R_G$ (left curves, free chain; right curves, adsorbed chain, $N = 1000$; particles of volumes equal to 1, 8, 27, and 64 are considered).

It is evident from Figure 17 that the probability of the coil penetration depends on the particle volume; the larger the volume the lower the probability that the particle will enter the coil. Irrespective of the particle volume, the probability of the segment−particle collision strongly increases after crossing a distance of approximately $2R_G$ from the coil center. Particles larger than the statistical segment length, but still small in comparison to the coil size (i.e., particles of volume $V = 8 \div 64$), will encounter the polymer segment before they reach the coil center. The presence of an irreversibly attached particle in the coil makes it easier for another particle to approach the coil center to a somewhat closer distance than that of the particle penetrating the undeformed coil. This can be explained by the coil contraction caused by irreversible attachment of the first particle.

The knowledge of the position of the site at which the particle encounters the polymer strand is insufficient, however, for prediction of the final conformation of the adsorbed polymer, because of the succeeding process of the chain reconformation. Pincus at al.,[17] who considered a system composed of a large macromolecule and small colloidal spheres, found that in the case of strong polymer adsorption the macromolecule wraps around a particle until saturation and then it goes on to bind another particle forming a necklace-like aggregate. However, if there is a large excess of particles in the system, one can expect the process of particle attachment to be much faster than the coil reconformation. Many particles can enter the coil simultaneously. The formation of intramolecular segment−particle−segment bridges can “freeze” the coil structure,[78] provided that the adsorption is strong. The structure of the resulting aggregates will be less ordered than that of necklaces. If particles are relatively large, they will be caught far away from the coil center; formation of a particle shell around the coil can be expected. The smaller the particles the smaller the shell diameter. Only for very small particles, whose size is comparable with the statistical segment length, the partial filling of the coil with particles is likely to happen.

In the case of weak adsorption limit, the adsorption is too weak to deform the coil; a macromolecule retains the free conformation, and only a short strand of the chain is involved in the adsorption process.[46,47] Thus, the structure of resulting particle-plus-polymer aggregates or—in other words—the arrangement of particles in the coil can be anticipated from analysis of the

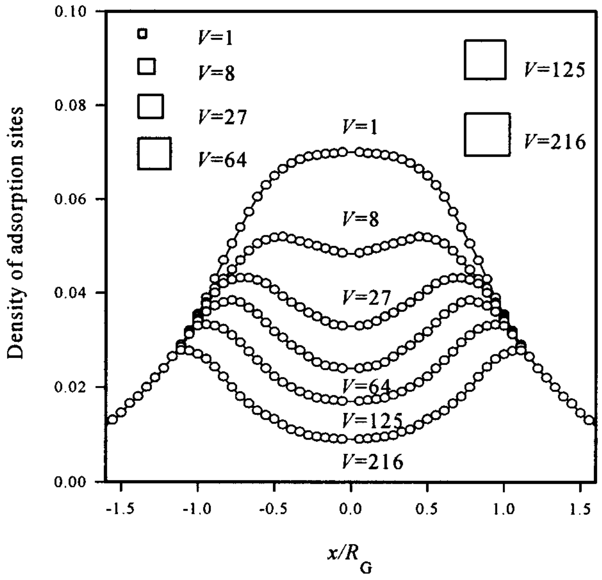

**Figure 18.** Density of adsorption sites vs the relative distance from the coil center, $x/R_G$ ($N = 1000$; particles of volumes equal to 1, 8, 27, 64, 125, and 216 are considered).

structure of the unperturbed coil. In Figure 18, the calculated distributions of adsorption sites for particles of different size are presented. As follows, in the case of very small particles (i.e., of the size comparable with the statistical segment length) the distribution exhibits a maximum at the coil center. For larger particles, distributions with two maxima, situated in a certain distance $R_A$ from the coil center, were obtained. The larger the particle the larger its distance from the coil center.

When the adsorption energy is small, the particle–polymer interaction takes the form of transient interaction,[47] which means that a particle can be detached from one macromolecular strand and become attached to another one. Since the particle can change its position in the coil, it can be expected to abide in a region of the highest adsorption site density. Small particles could preferably stay in the central region of the coil, whereas larger particles would rather occupy the regions laying at a certain distance from the coil center.

If a certain number of particles of the effective repulsion radius, $a_{\mathrm{eff}}$, small when compared to the coil size, enter the coil, the largest distance between the centers of weakly adsorbing particles is $2R_A$. This distance increases with the particle size, approaching limiting value of $2R_G$.

Analysis of the obtained distributions of adsorption sites allows also an estimation of the maximum number, $n_{\max}$, of particles that can be adsorbed on a single polymer molecule, provided that $a_{\mathrm{eff}} < R_A$ and the adsorption is weak. And so, if the size of particles is comparable with the statistical segment length, the particles and their electrostatic shells take up the central part of the coil and $n_{\max} \sim (R_G/a_{\mathrm{eff}})^3$. On the other hand, larger particles gather at a distance $R_A$ from the coil center; in the limiting case $R_A \approx R_G$, and hence $n_{\max} \sim (R_G/a_{\mathrm{eff}})^2$. A similar result, that is $n_{\max} = NL^2/a^2 \sim (R_G/a)^2$, where $a$ is the particle radius, was obtained by Klimov and Khokhlov,[79] by means of the free energy minimization method.

On the basis of the cavity distributions obtained, it is also possible to calculate the probabilities of free diffusion of a particle introduced into the coil. The probabilities can be calculated in the same way as those shown in Figure 17. The only difference is the initial position of the particle; in this case it is the position inside the coil. Thus, the probability that the particle will leave the coil without any collision with a polymer strand can be calculated from the equation:

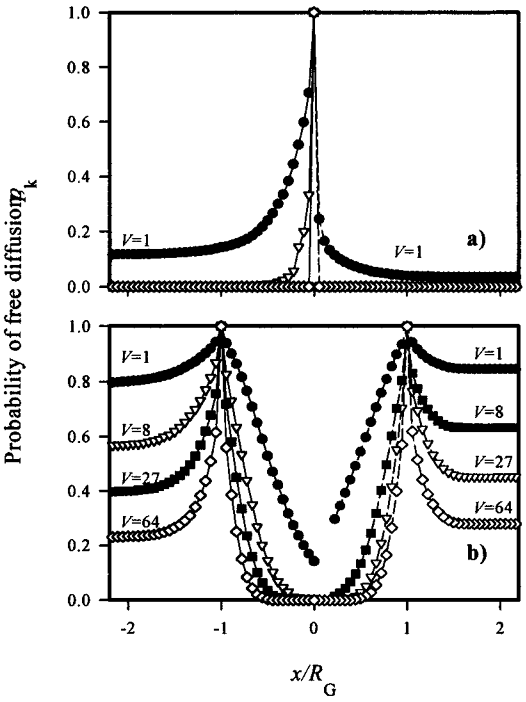

**Figure 19.** Probability of the particle escape from the coil, $p_k$, vs the relative distance from the coil center, $x/R_G$ (a, starting point at the coil center; b, starting point at the distance of $R_G$ from the coil center; left curves, unperturbed coil; right curves, coil perturbed by adsorbed particle, $N = 1000$; particles of volumes equal to 1, 8, 27, and 64 are considered).

$$p_k = \prod_{i=m}^{k} \rho_i \tag{23}$$

where $m$ is the initial distance of the particle from the coil center.

As follows from Figure 19, it is almost impossible for the particle to leave the coil in the collision-free way, and besides, the probability that the particle situated at the distance $m = R_G$ will leave the coil domain is very low. The reason is that the particle can diffuse in any direction; the direction toward the coil interior is also possible.

It is generally accepted that the polymer desorption from macroscopic surfaces and surfaces of large particles is a very slow process.[80–82] The reason is that a polymer molecule is attached to the surface with many contacts, and the desorption of the whole chain would require a simultaneous detachment of all these contacts. Such a process is statistically improbable.[81] Also, the energy required for desorption of an entire chain can be very high even though individual segments of the macromolecule can desorb quite easily.[82] However, in the case of very small particles, the adsorption energy can be very low, since the number of particle–polymer contacts is considerably reduced. Thus, the particle detachment can proceed quite readily. However, because of the high probability of the reattachment, the chance that the particle will leave the coil is very small. Hence, one can expect the effective desorption of a small particle from a large macromolecule to proceed very slowly.

## 4. Conclusions

The behavior of long linear polymer molecules in the presence of small colloidal particles was studied by means of the SAW chain on the cubic lattice.

The conformational entropies of coil perturbed by a nonadsorbing particle and by a particle attached to the chain were calculated. The extent of the entropy reduction caused by the chain attachment depends on the volume and shape of the particle and also on the chain length. A small particle induces only a local chain perturbation. The entropy-driven effect of pushing the particle toward the peripheries of the coil takes place. The minimum adsorption energy per the surface unit of particle, needed to outweigh the conformational entropy effect, depends on the particle size and the segment density in the adsorption layer. The dependence of this energy on the particle volume can go through a minimum. For very small particles, the adsorption energy can be insufficient to compensate the entropy loss although the adsorption on larger particles takes place.

A possibility of particle diffusion in the coil and possible structures of aggregates composed of a single macromolecule and one or a number of particles were analyzed in terms of the cavity and adsorption site distributions in the SAW coil. The coiled structure of very large polymer chains immersed in a good solvent can be penetrated by very small colloidal particles. When particles grow in size, their ability to penetrate the coil decreases. In the case of strong adsorption, formation of a layer of adsorbed polymer on the particle surface takes place; the adlayer thickness is determined by the particle size. The adlayer formation involves only a local coil perturbation. A simultaneous adsorption of many particles, except the smallest ones whose size is comparable with the statistical segment length, produces a particle shell around the coil. In the case of weak adsorption, extremely small particles are supposed to gather preferably in more densely segmented regions of the coil interior. When the particle size increases, the most probable particle position is at a certain distance from the center of the coil; the larger the particle the greater the distance. The largest distance approaches $2R_G$. The maximum number of particles that can be adsorbed on a single macromolecule depends on the particle size and is proportional to $R_G^3$, in the case of the smallest particles, and to $R_G^2$, for particles too large to enter the coil (but still small when compared to the coil size). The process of desorption of small particles from the coiled long chain is expected to proceed very slowly.

## References and Notes

(1) Fleer, G. J.; Cohen Stuart, M. A.; Scheutjens, J. M. H. M.; Cosgrove, T.; Vincent, B. *Polymers at Interfaces*; Chapman & Hall: London, 1993.
(2) Takahashi, A. *Polym. J.* **1991**, *5*, 715.
(3) Hone, D.; Hong, J.; Pincus, P. A. *Macromolecules* **1987**, *20*, 2543.
(4) Douglas, J. F. *Macromolecules* **1989**, *22*, 3707.
(5) Ball, R. C.; Blunt, M.; Barford, W. *J. Phys. A: Math. Gen.* **1989**, *22*, 2587.
(6) Baumgärtner, A.; Renz, W. *J. Phys. (Paris)* **1990**, *51*, 2641.
(7) Andelman, D.; Joanny, J. F. *Macromolecules* **1991**, *24*, 6040.
(8) Joanny, J. F.; Andelman, D. *Macromol. Chem., Macromol. Symp.* **1992**, *62*, 35.
(9) von Goeler, F.; Muthukumar, M. *J. Chem. Phys.* **1994**, *100*, 7796.
(10) Piculell, L.; Viebke, C.; Linse, P. *J. Phys. Chem.* **1995**, *99*, 17423.
(11) Stepanow, S.; Bauerschäfer, U.; Sommer, J. U. *Phys. Rev. E* **1996**, *54*, 3899.
(12) Yaman, K.; Pincus, P.; Solis, F.; Witten, T. A. *Macromolecules* **1997**, *30*, 1173.
(13) Kong, C. Y.; Muthukumar, M. *J. Chem. Phys.* **1998**, *109*, 1522.
(14) Cabane, B.; Duplessix, R. *J. Phys. (Paris)* **1982**, *43*, 1521.
(15) Sear, R. P. *J. Phys.: Condens. Matter* **1998**, *10*, 1677.
(16) Garvey, J. M.; Tadros, T. F.; Vincent, B. *J. Colloid Interface Sci.* **1976**, *55*, 440.
(17) Pincus, P. A.; Sandroff, C. J.; Witten, T. A. *J. Phys. (Paris)* **1984**, *45*, 725.
(18) Witten, T. A.; Pincus, P. A. *Macromolecules* **1986**, *19*, 2509.
(19) Marques, C. M.; Joanny, J. F. *J. Phys. (Paris)* **1988**, *49*, 1103.
(20) Baker, J. A.; Pearson, R. A.; Berg, J. C. *Langmuir* **1989**, *5*, 339.
(21) Birshtein, T. M.; Borisov, O. V. *Polymer* **1991**, *32*, 916.
(22) Pincus, P. *Macromolecules* **1991**, *24*, 2912.
(23) Aubouy, M.; di Meglio, J. M.; Raphaël, E. *Europhys. Lett.* **1993**, *24*, 87.
(24) Wijmans, C. M.; Leermakers, F. A. M.; Fleer, G. J. *Langmuir* **1994**, *10*, 1331.
(25) Cosgrove, T.; Griffiths, P. C.; Lloyd, P. M. *Langmuir* **1995**, *11*, 1457.
(26) Aubouy, M.; Raphaël, E. *Macromolecules* **1998**, *31*, 4357.
(27) Netz, R. R.; Joanny, J. F. *Macromolecules* **1999**, *32*, 9026.
(28) Buffle, J.; Wilkinson, K.; Stoll, S.; Fidella, M.; Zhang, J. *Environ. Sci. Technol.* **1998**, *32*, 2887.
(29) Wilkinson, K.; Balnois, E.; Leppard, G. G.; Buffle, J. *Colloids Surf., A* **1999**, *155*, 287.
(30) Andersson, K.; Larsson, H. *Nord Cellulosa* **1984**, *1*, 55.
(31) Wagberg, L.; Nordqvist, T. *Nord. Pulp Paper Res.* **1999**, *14*, 247.
(32) Swerin, A.; Ödberg, L.; Wagberg, L. *Colloids Surf., A* **1996**, *113*, 25.
(33) Janardhan, R.; Gedam, P. H.; Sampathkumaron, P. S. *J. Colloid Interface Sci.* **1990**, *140*, 391.
(34) Spinelli, J. H. *Adv. Mater.* **1999**, *10*, 1215.
(35) Kholkin, I. Y.; Viglazov, V. V.; Kind, V. B.; Mettee, H. D. *Appl. Biochem. Biotechnol.* **1999**, *82*, 135.
(36) Dickinson, E. *Int. Dairy J.* **1999**, *9*, 305.
(37) Gan, L. M.; Yeoh, K. W.; Chew, C. H.; Koh, L. L.; Tan, T. L. *J. Appl. Polym. Sci.* **1991**, *42*, 225.
(38) Bolto, B. A. *Prog. Polym. Sci.* **1995**, *20*, 987.
(39) Schmidt, C.; Bodmeier, R. *J. Controlled Release* **1999**, *57*, 115.
(40) Ha, H. K.; Shin, J. H.; Rha, S. E.; Lee, Y. S.; Park, K. B.; Lee, M. G.; Kim, P. N.; Auh, Y. H. *Radiology* **1999**, *211*, 197.
(41) Duro, R.; Souto, C.; Gomez-Amoza, J. L.; Martinez-Pacheco, R.; Concheiro, A. *Drug Dev. Ind. Pharm.* **1999**, *25*, 817.
(42) Odijk, T. *Physica A* **2000**, *278*, 347.
(43) Piculell, L.; Bregfeldt, K.; Gerdes, S. *J. Phys. Chem.* **1996**, *100*, 3675.
(44) Otsubo, Y. *Curr. Top. Colloid Interface Sci.* **1997**, *1*, 1.
(45) Cabane, B.; Wong, K.; Lindner, P.; Lafuma, F. *J. Rheol.* **1997**, *41*, 531.
(46) Wong, K.; Lixon, P.; Lafuma, F.; Lindner, P.; Aguerre Charriol, O.; Cabane, B. *J. Colloid Interface Sci.* **1992**, *153*, 55.
(47) Spalla, O.; Cabane, B. *Colloid Polym. Sci.* **1993**, *271*, 357.
(48) Larsson, A.; Wall, S. *Colloids Surf., A* **1998**, *139*, 259.
(49) Larsson, A.; Walldal, C.; Wall, S. *Colloids Surf., A* **1999**, *159*, 65.
(50) Stoll, S.; Buffle, J. *J. Colloid Interface Sci.* **1998**, *205*, 290.
(51) Chodanowski, P.; Stoll, S. *Colloid Polym. Sci.* **2000**, *278*, 406.
(52) Zhao, D.; Huang, Y.; He, Z.; Qian, R. *J. Chem. Phys.* **1996**, *104*, 1672.
(53) Munk, P. *Introduction to Macromolecular Science*; John Wiley & Sons: New York, 1989.
(54) Banaka, P. A.; Selser, J. C.; Wang, B.; Shenoy, D. K.; Martin, R. *Macromolecules* **1996**, *29*, 3956.
(55) Sykes, M. F.; Guttman, J.; Watts, M. G.; Robberts, P. D. *J. Phys. A* **1972**, *5*, 653.
(56) Le Guillon, J. C.; Zinn-Justin, J. *Phys. Rev. B* **1980**, *21*, 3976.
(57) Cifra, P.; Romanov, A. *Macromol. Chem.* **1986**, *187*, 2289.
(58) Meirovitch, H. *Macromolecules* **1983**, *16*, 249.
(59) Barber, M. N.; Guttman, A. J.; Middlemiss, K. M. *J. Phys. A: Math. Gen.* **1978**, *11*, 1833.
(60) Öttinger, H. C. *Macromolecules* **1985**, *18*, 9.
(61) Watts, M. G. *J. Phys. A* **1975**, *8*, 61.

(62) Wu, D.; Du, P.; Kang, J. *Sci. China B* **1997**, *40*, 1.
(63) Whittington, S. G. *J. Chem. Phys.* **1975**, *63*, 779.
(64) de Gennes, P. G. *C. R. Seances Acad. Sci., Ser. B* **1979**, *288*, 359.
(65) Odijk, T. *Macromolecules* **1996**, *29*, 1842.
(66) Sear, R. P. *Phys. Rev. E* **1997**, *56*, 4463.
(67) Grosberg, A. Y.; Khokhlov, A. R. *Giant Molecules*; Academic Press: San Diego, 1997.
(68) Rosenbluth, M. N.; Rosenbluth, A. W. *J. Chem. Phys.* **1955**, *23*, 356.
(69) Baumgärtner, A.; Muthukumar, M. Polymers in Disordered Media. In *Polymeric Systems*; Prigogine, I., Rice, S. A., Eds.; John Wiley & Sons: New York, 1996.
(70) Metropolis, N.; Rosenbluth, A. W.; Rosenbluth, M. N.; Teller, H. A.; Teller, E. *J. Chem. Phys.* **1953**, *21*, 1097.
(71) Verdier, P. H.; Stockmayer, W. H. *J. Chem. Phys.* **1962**, *36*, 227.
(72) Stockely, C.; Crabb, C. C.; Kovac, J. *Macromolecules* **1986**, *19*, 860.
(73) King, S. M.; Cosgrove, T. *Macromolecules* **1993**, *26*, 5414.
(74) Tanford, C. *Physical Chemistry of Macromolecules*; John Wiley & Sons: New York, 1961.
(75) Kuhn, W. *Kolloid Z.* **1934**, *68*, 2.
(76) Kurata, M.; Tsunashima, Y. *Polymer Handbook*, 3rd ed.; Brandrup, J., Immergut, E. H., Eds.; John Wiley & Sons: New York, 1989.
(77) Nowicki, W. *Colloids Surf., A* **2001**, *194*, 159.
(78) Stoll, S.; Buffle, J. *J. Colloid Interface Sci.* **1998**, *205*, 259.
(79) Klimov, D. K.; Khokhlov, A. R. *Kolloid. Zh.* **1991**, *33*, 1921.
(80) van de Ven, T. G. M. *Adv. Colloid Interface Sci.* **1994**, *48*, 121.
(81) Daoud, M.; Jannik, G. J. *J. Phys. (Paris)* **1976**, *37*, 473.
(82) Graessley, W. *Polymer* **1980**, *21*, 258.

MA010058D